FUDMA Journal of Sciences (FJS)
ISSN online: 2616-1370
ISSN print: 2645 - 2944
Vol. 6 No. 2, April, 2022, pp 208 - 220
DOI: https://doi.org/10.33003/fjs-2022-0602-962

NICKEL ADSORPTION ONTO SWEET DATTOCK SHELL: STATISTICAL ERROR FUNCTION MODELS AS PARAMETRIC ISOTHERM PREDICTORS

***Alsas, S. A., Zaharaddeen N. Garba & Sallau, M. S.**

Department of Chemistry, Ahmadu Bello University, Zaria, P.M.B 1044, Kaduna State, Nigeria.

*Corresponding authors' email: alsas4real@gmail.com +2347034662206

ABSTRACT

The speedy increase in the pollution of water bodies due to heavy metals discharged from tannery effluents is becoming a serious issue, calling for important measures to be taken to order to curtail water contamination. In this study, a low-cost adsorbent was prepared by carbonizing sweet dattock shell (Sd) for the removal of nickel (Ni) from tannery effluent. The two (Freundlich, Langmuir, Temkin) and three (Redlich Peterson, Sips, Toths) parameter isotherm models were used to fit the equilibrium data using linear regression methods by applying error functions in determine the best adsorption isotherm model. The scanning electron microscopy (SEM) and Fourier transform infrared (FTIR) were used to characterize the adsorbents. Sips and Langmuir were the best-fitted isotherm models for the process based on error functions. Chi-square error function predicted well for two-and three-parameter isotherm study having the lowest errors values. The FTIR showed a shift functional groups present at certain vibrations. The SEM affirmed irregular surface texture for the Sd with pore openings and whitish spots on the adsorbent. Also, Sd shell adsorption capacity proved efficient as an adsorbent for Ni removal from tannery effluents.

Keywords: Sweet dattock, adsorption, heavy metals, linear regression and error function

INTRODUCTION

The major characteristics of developed countries and the main target of developing countries are industrialization and urbanization (Dadhaniya *et al*, 2009). This though brought development but the economic solution to its disadvantages has become one of the challenging global problems (David *et al.*, 2000). To a larger extent, a high number of industrialization and urbanization have greatly increased the destruction of aquatic habitats through the release of industrial wastewater and domestic wastes (Demirbas *et al*, 2008). Poisonous metals posed a serious threat to the environment and people's health due to their high toxicity and bioaccumulation, not easily biodegradable in living cells, even at low concentrations (Hanna *et al*,. 2010, Renuga *et al.*, 2010) Pb (II), Ni (II), Cd and Cr (VI) ions have high solubility in the aquatic environment and thus can be absorbed by living organisms (Gonen and Serin, 2012), and when these metal ions are ingested beyond normal concentration, they generate serious health disorder (Garba *et al*., 2021; Garba *et al*., 2016; Garba *et al*., 2015)). It has also caused the biological cycling of toxic heavy metals (Nilanjana *et al*., 2008). A significant number of methods have been harnessed over the years to remove harmful metals from wastewater; such as chemical precipitation, reduction followed by electrochemical precipitation, chemical oxidation-reduction, ultrafiltration, reverse osmosis, solvent extraction, ion-exchange, electrodialysis, electrochemical coagulation and evaporation, (Regina *et al*., 2008; Ahmadpour *et al*., 2009). Most of these methods have amny disadvantages due to high cost, operational cost and generation of residual metal sludge after treatment (Demirbas *et al*., 2008; Gupta *et al*., 2007). These disadvantages, and together with the demand for more economical and efficient methods of metal recovery/removal from wastewater, have indulged inthe development of other separation techniques like adsorption (Adetokun *et al*., 2019; Afidah & Garba, 2016; Garba *et al*., 2021; Garba *et al*., 2019; Labaran *et al*., 2019; Surip *et al*., 2020; Tan *et al*., 2020; Xiao *et al*., 2020; Xiao *et al*., 2021) .Adsorption of heavy metals by adsorbents for reducing domestic and industrial or tannery effluents is achieved by green chemistry which minimizes the chemical sludge, regeneration of adsorbents and stability of metal recovery (Lofrano *et al*.,2012)

Deterium microcarpum is commonly known as sweet detar or sweet dattock. It is called by various names among the major tribes in Nigeria. For example, the Hausas and Igbos name it Taura and Ofo while the Yorubas referred to it as Ogbogbo. It is an under-utilized leguminous, having a twisted trunk and Wide-spreading crooked branches belonging to the subfamily *Caesalpinioideae*. It is widely found geographically in tropical western African countries such as Senegal, Sudan and Nigeria (Mann, 2003), but not much was reported on its capability to be used as an adsorbent after carbonizing. Therefore, the inventive aspect of this work is to investigate the adsorptive ability of carbonized and uncarbonized Sd for the removal of Ni from tannery effluents.

MATERIALS AND METHODS

The chemicals used in this research are of analytical grade, as such, they were used without any further purification. The sample was bought from Samaru market Zaria, Kaduna State, it was taken to the Department of Biological Sciences of the Ahmadu Bello University, Zaria, where it was identified as *Detarium microcarpum*. The pericarps were removed and de-shelled, then the shell was washed off with distilled water, air-dried for seven consecutive days to dehydrate it completely,

and then grounded to smaller forms with mortar and pestle (Musah *et al.,* 2016).

Preparation of adsorbents

The pre-treated sample was carbonized in a muffle furnace at a temperature of 300˚ C for 4 hrs. The sample material was allowed to cool to room temperature and washed with distilled water until a pH of 7 was obtained, the sample was then ground and sieved using 0.2 mm mesh. The sieved 0.2 mm particle size material for the carbonized sample was weighed and the particles were then dried in an oven at 25˚ C for 48hrs before being packed in an Air-tight sample bags for use (Abdulrazak *et al*., 2015; Garba, 2016).

Digestion of Sample

A measured amount of 20 mL of well-mixed sample was transferred to a 100 mL flask beaker in which 7.5 mL of concentrated HNO_3 and 2.5 mL of concentrated HCl were added to the sample. The sample was covered and heated on a hot plate at 90 – 95 ºC until the volume has been reduced to 10 mL. The beaker was then removed and allowed to cool. After cooling, the beaker was washed down with distilled water, filtered and the filtrate was transferred to a 20 mL container and adjusted to volume using distilled water (APHA, 2005).

Design of Experiment

The Central Composite Design (CCD) was used in designing the experiment with the help of Design-Expert software version 11.0.6 (Stat-Ease, Inc., Minneapolis, MN 55413, USA). Factors such as contact time, adsorbent dose and pH were varied and the response of the experiment was the removal percentage of the Ni metal ion from the collected tannery effluent (Garba *et al.,* 2016). The concentrations of the Ni were determined using Atomic absorption Spectrometer (AAS).

Adsorption Experiment

The sorption experiment was done by batch method. The method reported by Garba *et al.,* 2016 was adopted. An adsorption experiment was carried out in to study and evaluate the significance of variables on the percentage removal of Ni (II), Cd (II), Cr and Pb (II) according to the pH, time as well as the adsorbent dose as shown in table 3. The experiment was carried out at room temperature (25 ºC) on a mechanical shaker (Griffin flask shaker with serial number 76315) a 100 mL conical flask as the sample container. A significant amount of 50 mL solution of the tannery effluent was measured in the flask. The pH of the solution was adjusted to the required value throughout the experiment with 0.1 M NaOH and 0.1 M HNO_3. These gave only nitrate ions and sodium ions which are already in the medium without altering the chemistry of the ions of interest. Certainly weighed grams of the adsorbent were transferred into each of these conical flasks; each set was agitated on the shaker at the a different time, And the samples were filtered, digested according to the APHA method (2005) and analysed for residual metals concentrations. The percentage removals were obtained using the expression below

$$\%Removal = \frac{(C_o - C_e)}{C_o} \times 100 \qquad (1)$$

where C_o = initial concentration, C_e= final concentration

The gram of a particular metal adsorbed per unit gram of adsorbent otherwise known as adsorption capacity after a given time was calculated using the expression below:

$$q_t = \frac{(C_o - C_e)V}{W} \qquad (2)$$

where V= Volume of the solution, W= Mass of the adsorbent

Equilibrium adsorption isotherm models

Adsorption isotherms explain adsorbed Molecules'distribution between the solid phase and the liquid phase when the adsorption process reaches an equilibrium state. To fit the experimental data, the isotherm models used include two-parameters (Freundlich, Langmuir, Temkin) and three-parameters (Redlich-Peterson, Sips and Toth) isotherm models.

Error functions

Some of the error functions used are (sum of squares of the errors, residual root mean square error, average relative error, coefficient of determination, the standard deviation of relative errors, non-linear chi-square test hybrid functional error, normalized standard deviation, the sum of absolute error and Spearman's correlation coefficient) for this study. Non-linear chi-square test is calculated via summation of squares differences between calculated and experimental data with each squared difference divided by its corresponding value. A sum of squares of the errors is obtained by summing the squares of the difference between experimental and calculated values for the number of data points considered. The residual root means square error is used to find an equilibrium model with optimal magnitude. The Hybrid functional error was developed as an advancement on the sum of squares errors (SSE) at low concentrations obtained by dividing SSE value with the experimental solid-phase concentration with an inclusive divisor in the system as a term for the number of degrees of freedom (Data points number the number of parameters within the isotherm equation). The algorithms for the simulation of linear isotherm models using error functions were presented as Fig. 1.

Table 1: Equilibrium Isotherm Models used for the Heavy Metals Uptake onto Sd

Models	Linear Models	Plot	Slope and Intercept	References
	Two-Parameter Isotherms			
Freundlich	$\log q_e = \log K_F + \frac{1}{n}\log C_e$	log q_e vs log C_e	Slope = 1/n, Intercept = log K_F	Piccin *et. al.* (2011)
Langmuir	$\frac{C_e}{q_e} = \frac{1}{K_L q_{\max}} + \frac{C_e}{q_{\max}}$ $R_L = \frac{1}{1+K_L C_o}$	$\frac{C_e}{q_e}$ vs C_e	Slope = $\frac{1}{q_{\max}}$, Intercept = $\frac{1}{(K_L q_{\max})}$	Langmuir (1918)
Temkin	$q_e = b_T InA_T + b_T InC_e$	q_e vs $ln\ C_e$	Slope = b_T, Intercept = $b_T InA_T$	Temkin *et. al.* (1940)
	Three-Parameter Isotherms			
Redlich-Peterson	$In\left(K_{RP}\frac{C_e}{q_e}-1\right) = \beta_{RP} InC_e + Ina_{RP}$	$In\left(K_{RP}\frac{C_e}{q_e}-1\right)$ vs InC_e	Slope = β_{RP}, Intercept = Ina_{RP}	Redlich *et. al.* (1959)
Sips	$In\left(\frac{q_e}{q_m-q_e}\right) = \frac{1}{n}In(C_e) + In(b_s)^{\frac{1}{n}}$	$In\left(\frac{q_e}{q_m-q_e}\right)$ vs InC_e	Slope = $\frac{1}{n}$, Intercept = $In(b_s)^{\frac{1}{n}}$	Sips (1948)
Toth	$In\left(\frac{q_e^{n_t}}{q_m^{n_t}-q_e^{n_t}}\right) = n_t InC_e + n_t InK_t$	$In\left(\frac{q_e^{n_t}}{q_m^{n_t}-q_e^{n_t}}\right)$ vs InC_e	Slope = n_t, Intercept = $n_t InK_t$	Toth (1971)

q_e (mg g^{-1}): experimental adsorption capacity of Sd adsorbent at equilibrium, K_F (mg g^{-1}) (L $mg^{-1})^{1/n}$: Freundlich isotherm constant related to the sorption capacity, C_e (mg L^{-1}): heavy metals adsorbate equilibrium concentration, n: a constant which gives an idea of the grade of heterogeneity, K_L (L mg^{-1}): Langmuir constant related to the affinity of the binding sites and the energy of adsorption, C_o (mg L^{-1}): highest initial adsorbate concentration, R_L: dimensionless Langmuir equilibrium parameter, q_m (mg g^{-1}): maximum monolayer adsorption capacity of the Sd adsorbent, R (8.314 $Jmol^{-1}$): universal gas constant, T (°K): absolute temperature, b_T (J mol^{-1}): Temkin constant related to heat of adsorption, A_T (L mg^{-1}): equilibrium binding constant corresponding to the maximum binding energy, E (kJ mol^{-1}): mean free energy of adsorption and K_{RP} (L/g): Redlich–Peterson isotherm constant, a_{RP} (L/mg): Redlich–Peterson isotherm constant, β: Redlich–Peterson exponent which lies between 0 and 1, b_s: Sips isotherm constant related to energy of adsorption, K_t: Toth model adsorption isotherm constant, n_t: Toth model exponent, b_K: Khan model constant, a_K: Khan model exponent.

Table 2: List of Error Functions

Error Function	Abbreviation	Model	Reference
Nonlinear chi-square test	χ^2	$\chi^2 = \sum_{i=1}^{n} \frac{\left(q_{e,\exp} - q_{e,calc}\right)^2}{q_{e,\exp}}$	Ho *et al*. 2006; Boulinguiez *et al*. 2008
Sum of squares of the errors	*SSE*	$SSE = \sum_{i=1}^{n} \left(q_{e,\exp} - q_{e,calc}\right)^2$	Kumar *et al*. 2006
Average relative error	*ARE*	$ARE = \frac{100}{n} \sum_{i=1}^{n} \left\lvert \frac{q_{e,\exp} - q_{e,calc}}{q_{e,\exp}} \right\rvert$	Subramanyam *et al*. 2014
Residual root mean square error	*RMSE*	$RMSE = \sqrt{\frac{1}{n-2} \sum_{i=1}^{n} \left(q_{e,\exp} - q_{e,calc}\right)^2}$	Vijayaraghavan *et al*. 2006
Standard deviation of relative errors	S_{RE}	$S_{RE} = \sqrt{\frac{\sum_{i=1}^{n} \left[\left(q_{e,\exp} - q_{e,calc}\right) - ARE\right]^2}{n-1}}$	Boulinguiez *et al*. 2008
Normalized standard Deviation	*NSD*	$NSD = \Delta q(\%) = 100 \sqrt{\frac{1}{n-1} \sum_{i=1}^{n} \left(\frac{q_{e,\exp} - q_{e,calc}}{q_{e,\exp}} \right)^2}$	Wang *et al*. 2010
Hybrid functional Error	*HYBRID*	$HYBRID = \frac{100}{(n-p)} \sum_{i=1}^{n} \frac{\left(q_{e,\exp} - q_{e,calc}\right)}{q_{e,\exp}}$	Ng *et al*. 2002
Sum of absolute error	*EABS*	$EABS = \sum_{i=1}^{n} \left\lvert q_{e,\exp} - q_{e,calc} \right\rvert$	Ng *et al*. 2003

$q_{e,\exp}$ (mg g^{-1}): value obtained from the batch experiment, $q_{e,\text{calc}}$ (mg g^{-1}): calculated value from the isotherm for corresponding $q_{e,\exp}$, $\overline{q}_{e,calc}$ (mg g^{-1}): mean of $q_{e,\text{calc}}$, n: number of experimental data points, and p: number of parameters in the respective model.

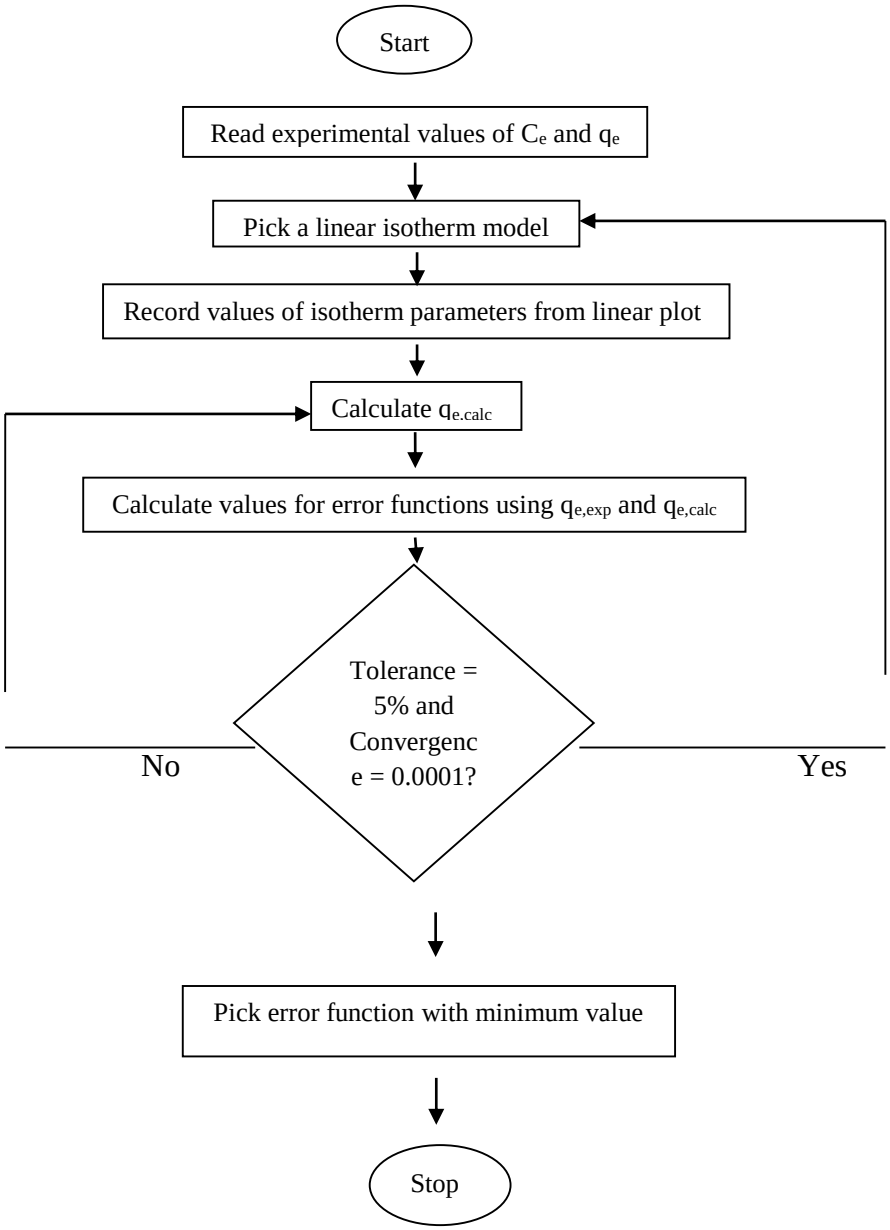

Figure 1**:** Algorithm for Linear Isotherm Models Regression using Error Functions (Popoola *et al., 2019*)

RESULTS AND DISCUSSION

Table 3: Design Matrix of the Experimental Runs and the percentage removal of Ni

Run	Ph	Adsorbent dose (g)	Contact Time (min)	Ni removal (%)
1	6	0.55	24	99.6444
2	6	0.55	14	98.6444
3	4	0.3	20	99.7444
4	6	0.13	14	99.3424
5	8	0.3	8	93.6203
6	8	0.8	8	93.6203
7	6	0.55	14	98.6324
8	8	0.3	20	94.1763
9	9	0.55	14	87.1763
10	6	0.55	14	98.6203
11	6	0.55	3.9	99.6324
12	6	0.97	14	98.6324
13	4	0.8	8	98.1763
14	8	0.8	20	93.6203
15	3	0.55	14	96.687
16	6	0.55	14	98.6203
17	6	0.55	14	98.1763
18	4	0.3	8	99.7407
19	6	0.55	14	98.7407
20	4	0.8	20	99.6369

The table above shows the adsorption experiment which was carried out in to tudy and evaluate the gnificance of variables on the percentage removal of Ni according to the pH, time as well as the adsorbent dosage.

Material characterization

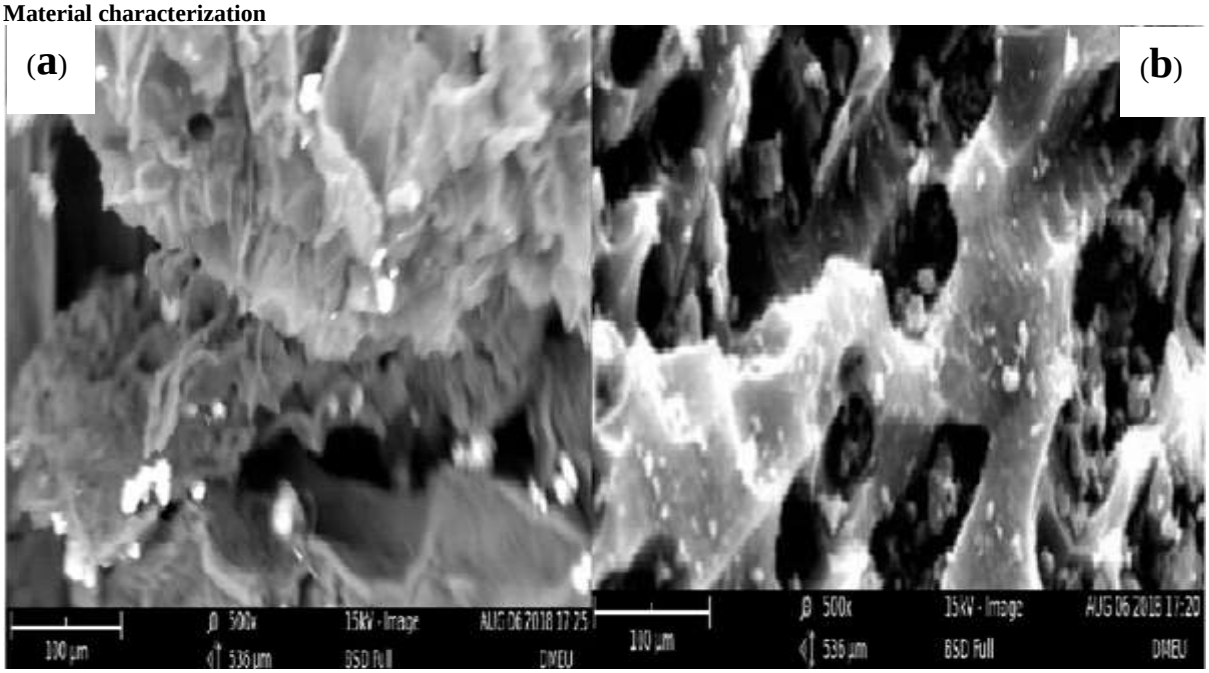

Figure 3: SEM micrograph (a) carbonized and (b) carbonized Sd

The image of the carbonized (×500 magnification) Sd as shown in plate 3(b) shows more whitish spots appearing as flakes and grain-like structures on the surface of the Sd than on the micrograph of the uncarbonized Sd in figure 3(a) which is a good adsorbent property for an adsorption process. Such porosities and irregularities were also reported on adsorbents prepared from coconut shells as obtained by Song *et al*. (2014).

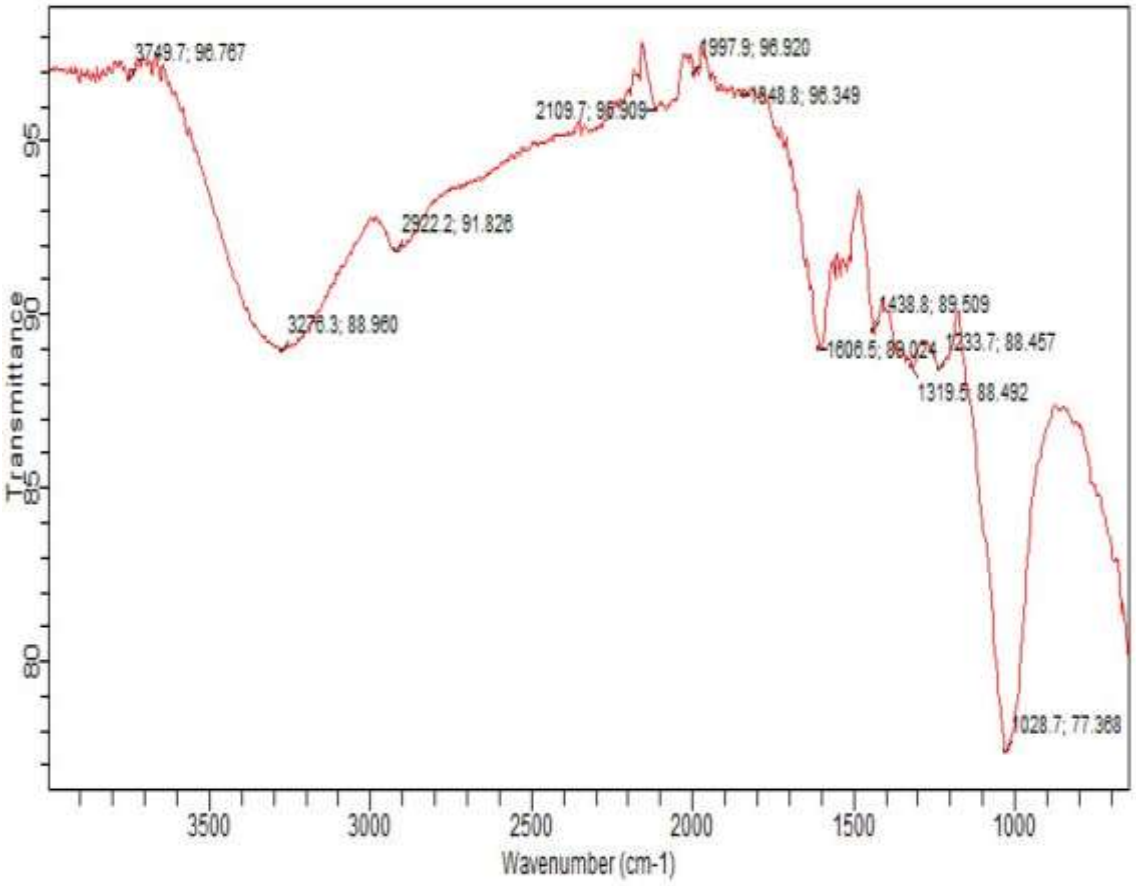

Figure 4: FTIR spectra of Sd

From the IR spectra of the Sd presented in Fig 4. There is the presence of –OH group which is attributed to the Vibration at 3276 cm^{-1}. Strong vibration at 2922 cm^{-1} shows the presence of C-H of alkanes while vibration at 1606 cm^{-1} potrays the existence of C=C and lower vibration at 1028 cm^{-1} identified C-O as the functional group in the adsorption process(Absorption table, 2014; Spectroscopic tools, 2018).

(a)

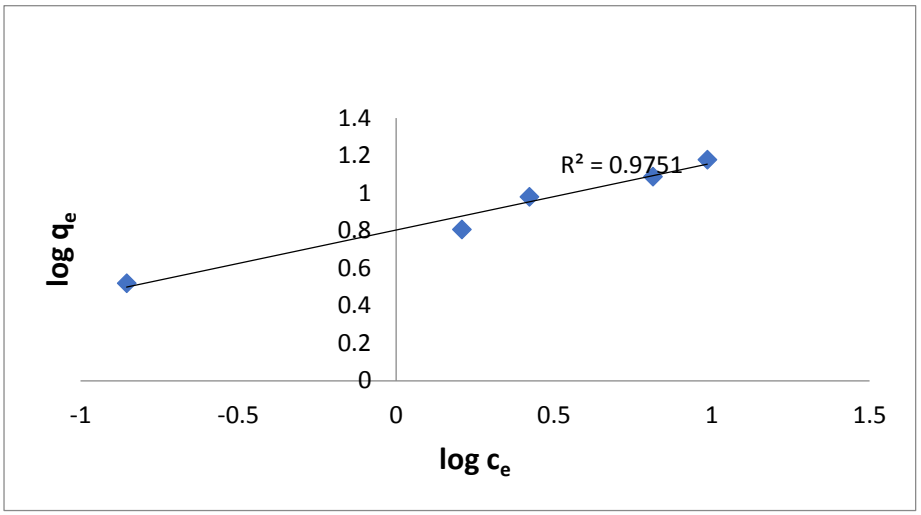

(b)

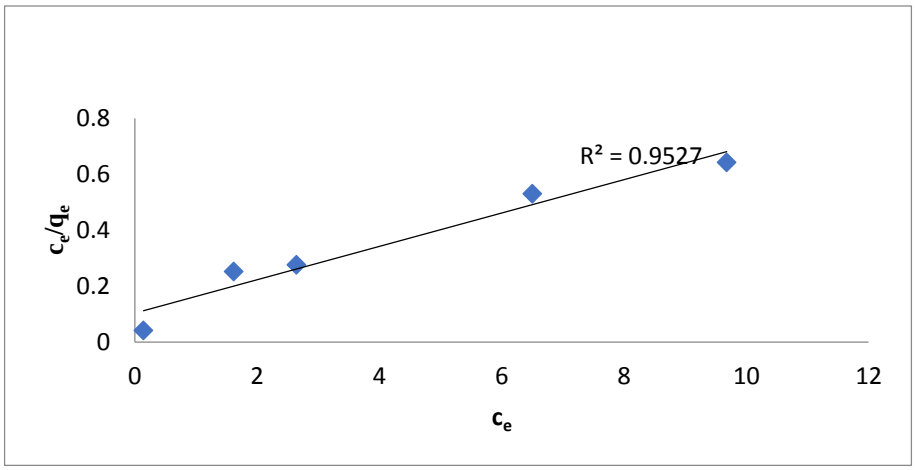

(c)

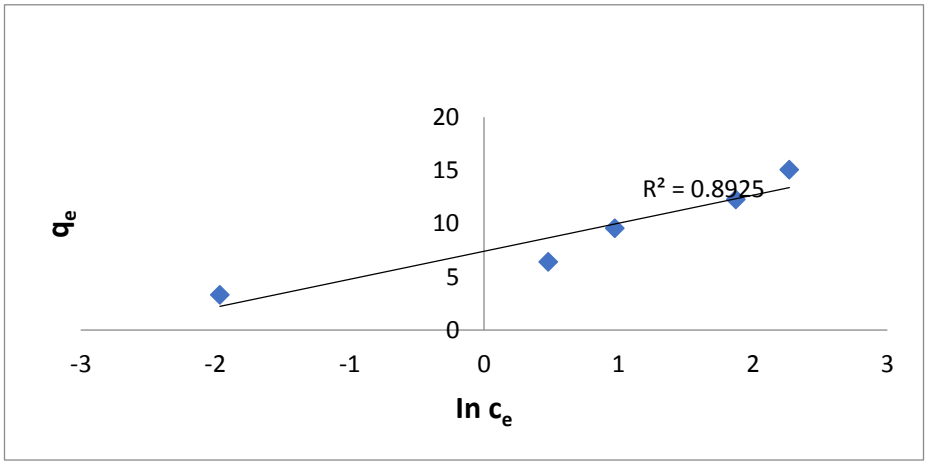

Figure 5: Linearized (a) Langmur (b) Freundlich and (c) Temkin isotherm plots for Nickel adsorption onto which adsorbent carbonised Sd

(a)

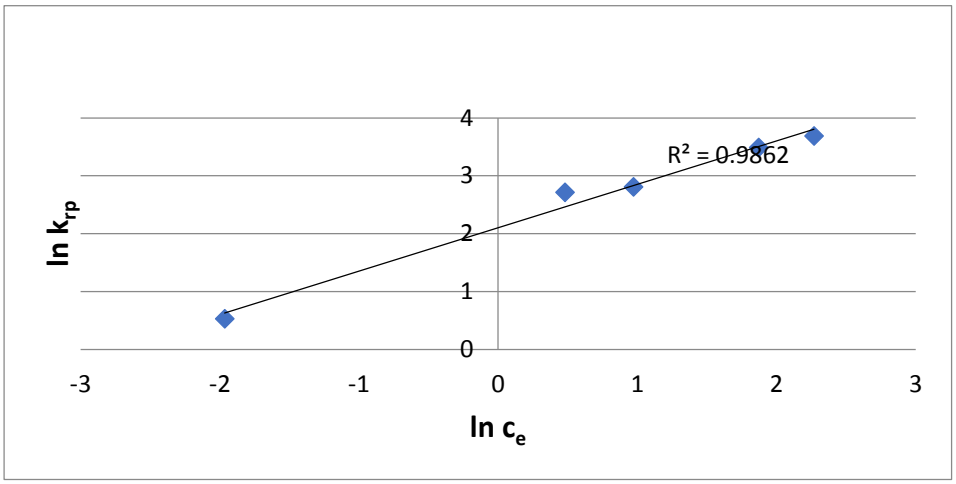

(b)

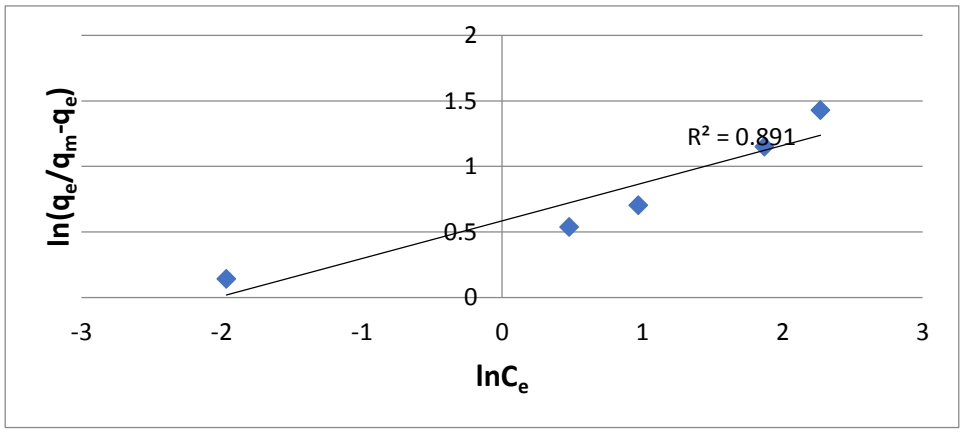

(c)

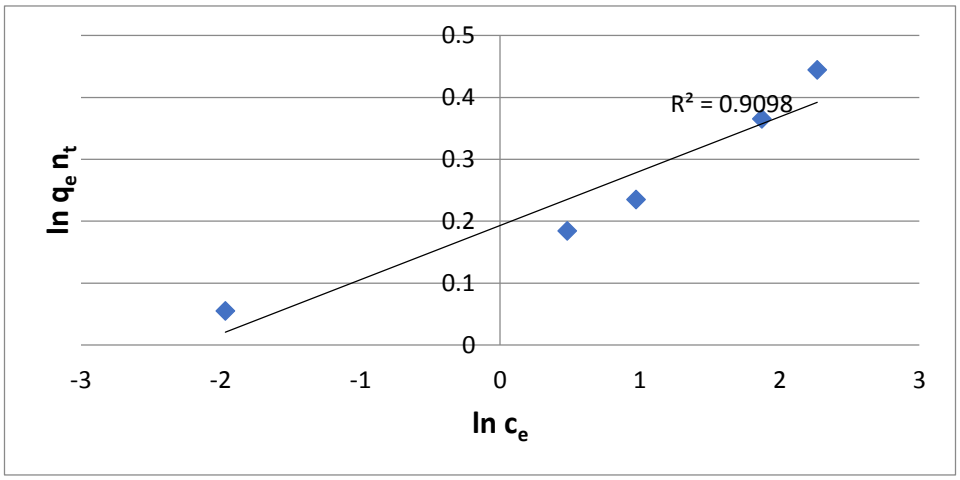

Figure 6: Linearized (a) Redlich-Peterson (b) Sips and (c) Toths isotherm plots for Nickel adsorption onto which adsorbent carbonized Sd

Linear Regression of two-Parameter Isotherm Models

Fig 5 a, b and c revealed linear plots for all the linearized two-parameter isotherm models for Ni adsorption on Sd. Among the investigated two-parameter isotherms, R^2 value of 0.8925 was obtained for Temkin isotherm while R^2 values for Langmuir and Freundlich isotherms were 0.9751 and 0.9527 as obtained respectively in (fig 5). A similar result result had been presented elsewhere (Anilkumar *et al* 2016).

Conforming results were revealed by Kooh *et al.,* 2016 and Hamzaoui *et al.,* 2018 while Nethaji *et al.,* 2013 found a contrary result.

Linear regression of three-parameter isotherm models

Fig 6. a, b and c showed linear plots for all the linearized three-parameter isotherm models for Ni adsorption on Sd. The R-p isotherm fitted well for the adsorption of Ni using Sd with R^2 value of 0.9862 while the R^2 values for Toth and Sips isotherms were 0.9098 and 0.891, respectively. The similiar results had been showed elsewhere (Dahri *et al.,* 2017).

Table 4: Error Functions for Linear Regression of Nickel

Models	Error functions SSE	X^2	ARE	RMSE	SRE	NSD	HYBRID	EABS
Two-parameters isotherm models								
Freundlich	8.2777	1.3647	12.8614	2.1538	8.7901	21.5713	25.7228	4.4254
Langmuir	9.0902	1.2834	27.0343	2.1319	16.6466	39.5111	54.0686	6.1444
Temkin	1399.2	129.861	209.408	26.45	112.881	218.475	418.82	77.182
Three-parameters isotherm models								
R-P	0.641	5.609	11.692	1.675	15.025	16.906	6.038	3.888
Sips	0.657	5.100	12.849	1.597	16.709	18.189	51.396	3.796
Toth	38.528	421.380	115.562	14.515	125.100	119.444	462.247	42.336

Table 4 presented the values obtained from the simulation of error functions using linearized isotherm models of two and three parameters. The result showed Langmuir isotherm model to be the best two-parameter model fit for heavy metal adsorption from tannery effluent using Sd having the lowest values for the error functions while Sips is the best three-parameter isotherm model that best describes the adsorption process with lowest error functions values. The sequence of best fit for two-parameter isotherm models is Langmuir, Freundlich and Temkin as presented in Table 4 while the best is Sips, R-P and Toth for three-parameter models. Evidently, of all the error functions used, chi-square was the best error method that can accurately determine isotherm model parameters as it gave the lowest error value of 1.2834 and 5.100 for two and three- parameters isotherm models as obtained in Table 4 respectively (Neibi *et al.,* 2008). The results from error functions were also confirmed with the linear regression analysis for the isotherm models as both Langmuir and Sips were shown to be the best model describing heavy metal adsorption from tannery effluents using Sd adsorbents having the lowest error values. Previous research have also revealed similar results. (Bera *et al.,* 2013 and Hamdaoui *et al.,* 2007**)**

Table 5: Two-Parameter Adsorption Isotherm Constants and R^2 Values for Ni Uptake on Sd

Isotherms	Elements
	Ni
Langmuir	
Q_{max} (mg g^{-1})	16.716
K_L(L mg^{-1})	1.714
R_L	0.028
R^2	0.9751
Freundlich	
K_F [(mg g^{-1})(L mg $g^{-1})^{1/n}$]	6.338
1/n	0.352
R^2	0.9527
Temkin	
A_T	16.493
b_T	2.608
R^2	0.8925

Table 5 shows the two two-parameter adsorption isotherm constants and R^2 values for Ni adsorption on Sd. The langmuir has R^2 value of 0.9527 while Freundlich and Temkin have 0.9751 and 0.8925 respectively. The Best-fitted adsorption isotherm model here is Langmuir followed by Freundlich and Temkin respectively due to their lowest error values as shown in table 4.

Table 6: Three-Parameter Adsorption Isotherm Constants and R^2 Values for Ni Uptake on Sd

Isotherms	**Elements**
	Ni
Redlich-peterson	
K_{RP} (L g^1)	63.71
A_{RP} (L mg^1)	8.044
β_{RP}	0.747
R^2	0.9862
Sips	
q_{max} (mg g^{-1})	6.156
1/n	0.285
b_s (L g^1)	1.791
R^2	0.8911
Toths	
q_{max} (mg g^{-1})	55.14
n_t	0.084
K_t	9.058
R^2	0.9098

Table 6 shows the three three-parameter adsorption isotherm constants and R^2 values for Ni adsorption on Sd .The Sips has R^2 value of 0.891 while Redlich-peterson and Toths have 0.9862 and 0.9098 respectively. The best fitted adsorption isotherm model here is Sips followed by Redlich-peterson and Toths respectively due to their lowest error values as shown in table 4.

CONCLUSION

Linear regression of isotherm models having two and three parameters hasbeen studied using a several of error functions for Ni removal from tannery effluents using Sweet dattock shells (Sd). In two and three parameters, Langmuir and Sips used fitted well for Ni adsorption from tannery effluents using Sd. Chi-square (χ^2) predicted well for Langmuir, Freundlich and Temkin isotherm models for heavy metals adsorption onto Sd. The images from SEM showed irregular surface texture with pore openings and whitish spots confirming Sd efficacy for the adsorption process. The FTIR result showed the functional group present at different vibrations.

REFERENCES

Abdulrazak S., Hussaini K. and Sani H. M. (2017). Evaluation of removal efficiency of heavy metals by low-cost activated carbon prepared from African palm fruit. Applied Water Science, 7(6), 3151–3155. Doi: https://doi.org/10.1007/s13201016-0460-x

Absorption table. (2014). Infrared Spectroscopy Absorption Table. Retrieved September 10, 2018 from https://chem.libretexts.org/Reference/ReferenceTables/Spectroscopic-Parameters/InfraredSpectroscopyAbsorptionTable

Adetokun, A.A., Uba, S., Garba, Z.N. 2019. Optimization of adsorption of metal ions from a ternary aqueous solution with activated carbon from Acacia senegal (L.) Willd pods using Central Composite Design. J. King Saud Univ. - Sci., Article in Press, https://doi.org/10.1016/j.jksus.2018.12.007.

Afidah, A.R., Garba, Z.N. 2016. Efficient adsorption of 4-Chloroguiacol from aqueous solution using optimal activated carbon: Equilibrium isotherms and kinetics modeling. J. Assoc. Arab Universities Basic Appl. Sci., 21, 17-23.

Ahmadpour A, Tahmasbi M, Rohani BT & Amel BJ 2009. Rapid removal of cobalt ion fromaqueous solutions by almond green hull. J. Hazardous Materials,166:925-930.

Anilkumar B., Chitti N. B. and Kavitha G. (2016). Biosorption of zinc on to gracilaria corticata (red algae) powder and optimization using central composite design. Journal of Applied Science and Engineering Methodologies, 2(3), 412-425.

Bera, A., T. Kumar, K. Ojha and A. Mandal, (2013). Adsorption of surfactants on sand surface in enhanced oil recovery: Isotherms, kinetics and thermodynamic studies. Applied Surf. Sci., 284: 87-99.

Boulinguiez, B., P. Le Cloirec and D. Wolbert, 2008. Revisiting the determination of langmuir parameters-application to tetrahydrothiophene adsorption onto activated carbon. Langmuir, 24: 6420-6424.

Dadhaniya PV, Patel AM, Patel MP & Patel RG 2009. A new cationic poly (1-vinyl-v3-ethylImidazolium iodide), P (VEII) hydrogen for the effective removal of chromium (VI) from aqueous solution. J. Macromol. Sci. Part A: Pure and Appl. PolymerChem., 46: 447-454.

Dahri, M.K., Kooh, .M.R.R. and Lim, L.B.L., (2017). Adsorption characteristics of pomelo skin toward toxic Brilliant Green dye. Scientia Bruneiana, 16: 49-56.

David H. (2000). Modern Analytical Chemistry. USA: McGraw-Hill

Demirbas E, Kobya M & Konukmanc AES 2008. Equilibrum studies for the Almond shell activated carbon adsorption of Cr (VI) from aqueous solution.J. Hazaardous Materials, 154:787-794.

Dubinin, M.M., 1960. The potential theory of adsorption of gases and vapors for adsorbents with energetically nonuniform surfaces. Chem. Rev., 60: 235-241.

Garba Z. N., Idris B., Ahmad G. and Aisha Y.L. (2016). Optimization of adsorption conditions using central composite design for the removal of copper (II) and lead (II) by defatted papaya seed. Karbala International Journal of Modern Science, 2, 20-28.-141.

Garba, Z.N., Abdullahi, A.K., Haruna, A., Gana, S.A. 2021. Risk assessment and the adsorptive removal of some pesticides from synthetic wastewater: a review. Beni-Suef Univ. J. Basic Appl. Sci., 10, https://doi.org/10.1186/s43088-021-00109-8.

Garba, Z.N., Bello, I., Galadima, A., Aisha, Y.L. 2016. Optimization of adsorption conditions using central composite design for the removal of copper (II) and lead (II) by defatted papaya seed. Karbala Intl J Modern Sci 2, 20-28.

Garba, Z.N., Hussin, M.H., Galadima, A., Lawan, I. 2019. Potentials of Canarium schweinfurthii seed shell as a novel precursor for CH3COOK activated carbon: statistical optimization, equilibrium and kinetic studies. Appl. Water Sci., 9(31), 1-13.

Garba, Z.N., Ubam, S., Babando, A.A., Galadima, A. 2015. Quantitative assessment of heavy metals from selected tea brands marketed in Zaria, Nigeria. J. Phys. Sci., 26(1), 43-51.

Gonen F & Serin SD 2012. Adsorption study on orange peel: Removal of Ni (II) ions from aqueous solution. African Journal Biotech.,11(5):1250-1258.

Gupta, V.K. and Rastogi, A. (2007). Biosorption of lead from aqueous solutions by green algae spirogyra species. Kinetics and equilibrum studies. J.Colloid Interface Sci., 296: 59 – 63.

Hamzaoui, M., B. Bestani and N. Benderdouche, (2018). The use of linear and nonlinear methods for adsorption isotherm optimization of basic green 4-dye onto sawdust-based activated carbon. J. Mater. Environ. Sci., 9: 1110-1118.

Hanan EO, Reham KB & Hanan FA 2010. Usage of some agricultural by-product in the removal of some heavy metals from industrial waste water. J. Philology, 2(3):51-62.

Ho, Y.S. Porter, J.F. Mckay, G. Equilibrium isotherm studies for the sorption of divalent metal ions onto peat: copper, nickel and lead single component systems, Water Air Soil Pollut. 141 (2002) 1–33.

Kooh, M.R.R., M.K. Dahri and L.B. Lim, (2016). The removal of rhodamine B dye from aqueous solution using Casuarina equisetifolia needles as adsorbent. Cogent Environ. Sci., Vol. 2. 10.1080/23311843.2016.1140553.

Kumar P. P., Kumar P. Y. and Rao B. V. (2017). Optimization of zinc(ii) biosorption on to Boodlea struveiodes (marine algae) by central composite design. Rasayan Journal of Chemistry, 10(3), 1025-1036.

Labaran, A.N., Zango, Z.U., Armayau, U., Garba, Z.N. 2019. Rice husk as biosorbent for the adsorption of methylene blue. Sci. World J., 14, 66-69.

Langmuir, I., 1918. The adsorption of gases on plane surfaces of glass, mica and platinum. J. Am. Chem. Soc., 40: 1361-1403

Lofrano G., Brown J. and Feo G. D. (2012). Green practices to save our precious "water resource". In Sharma K. S. and Shangai R. (Ed.), Advances in Water Treatment and Pollution Prevention (37). Dordrecht: Springer Science Business Media. Doi:10.1007/978-94-007-4204-8_5

Mann A, Muhammad G & Abdulkadir NU 2003. Medicinal and economical plants of Nupeland, p. 53.

Musah M, Yisa J, Mann A, Suleiman MAT & Aliyu A 2016. Preparation and characterization of mesoporous functionalized activated carbon from Bombax buonopozense calyx.Am. J. Innovative Res. and Appl. Sci., 3(2):90-97

Ncibi, M.C., (2008). Applicability of some statistical tools to predict optimum adsorption isotherm after linear and non-linear regression analysis. Journal Hazardeous. Materials., 153: 207-212.

Nethaji, S., A. Sivasamy and A.B. Mandal, (2013). Adsorption isotherms, kinetics and mechanism for the adsorption of cationic and anionic dyes onto carbonaceous particles prepared from Juglans regia shell biomass. International Journal of Environmental Science Technology., 10: 231-242.

Ng, J.C.Y., W.H. Cheung and G. McKay, 2002. Equilibrium studies of the sorption of Cu(II) ions onto chitosan. J. Colloid Interface Sci., 255: 64-74.

Ng, J.C.Y., W.H. Cheung and G. McKay, 2003. Equilibrium studies for the sorption of lead from effluents using chitosan. Chemosphere, 52: 1021-1030.

Nilanjana, D., Karthika, P., Vimala, R. and Vinodhini, V. (2008). Use of natural products as biosorbent of heavy metals. An overview. Natural Product Radiance, 7(2): 133 – 138.

Piccin, J.S., G.L. Dotto and L.A.A. Pinto, 2011. Adsorption isotherms and thermochemical data of FD&C Red nE40 binding by chitosan. Braz. J. Chem. Eng., 28: 295-304.

Popoola T.F , Adeyinka S.Y, Olusola A.A and Mayowa A.L, Brilliant Green Dye Sorption onto Snail Shell-rice Husk: Statistical and Error Function Models as Parametric Isotherm Predictors ISSN 1994-7887 65.80.2019.

Regina E, Onyewachi OA & Vivano OA 2008. Removal of some metal ions from aqueous solution using orange mesocarp. African Journal of Biotechnology., 7(17): 3073 – 3076.

Regina E, Onyewachi OA & Vivano OA 2008. Removal of some metal ions from aqueous solution using orange mesocarp. African J. Biotech., 7(17): 3073 – 3076.

Renuga DN, Mansusha K & Latitha P 2010. Removal of Hexavalent chromium from aqueous solution using an eco-friendly activated carbon adsorbent. Pelagia Res Library Advancesin Appl. Sci. Res., 1(3): 247 – 254.

Sips, R., 1948. On the structure of a catalyst surface. J. Chem. Phys., 16: 490-495.

Song C., Wu S., Cheng M., Tao P., Shao M. and Gao G. (2014). Adsorption studies of coconut shell carbons prepared by koh activation for removal of lead(ii) from aqueous solutions. Sustainability, 6, 86-98.

Spectroscopic tools. (2018). Accessed on September 10, 2018 from http://www.science-and-fun.de/tools/

Subramanyam, B. and A. Das, 2014. Linearised and non-linearised isotherm models optimization analysis by error functions and staqatistical means. J. Environ. Health Sci. Eng., Vol. 12. 10.1186/2052-336X-12-92.

Surip, S.N., Abdulhameed, A.S., Garba, Z.N., Syed-Hassan, S.A., Ismail, K., Jawad, A.H. 2020. H2SO4-treated Malaysian low rank coal for methylene blue dye decolourization and cod reduction: Optimization of adsorption and mechanism study. Surf. Interf., 21, 100641.

Tan, C.H.C., Sabar, S., Haafiz, M.K.M., Garba, Z.N., Hussin, M.H. 2020. The improved adsorbent properties of microcrystalline cellulose from oil palm fronds through immobilization technique. Surf. Interf., 20, 100641.

Temkin, M.J. and V. Pyzhev, 1940. Kinetics of ammonia synthesis on promoted iron catalysts. Acta Physicochim. URSS, 12: 217-222.

Toth, J., 1971. State equation of the solid-gas interface layers. Acta Chim. Hung., 69: 311-328.

Vijayaraghavan, K., T.V.N. Padmesh, K. Palanivelu and M. Velan, 2006. Biosorption of nickel(II) ions onto Sargassum wightii: Application of two-parameter and three-parameter isotherm models. J. Hazard. Mater., 133: 304-308.

Wang, L., J. Zhang, R. Zhao, Y. Li, C. Li and C. Zhang, 2010. Adsorption of Pb(II) on activated carbon prepared from Polygonum orientale Linn.: Kinetics, isotherms, pH and ionic strength studies. Bioresour. Technol., 101: 5808-5814.

Xiao, W., Garba, Z.N., Sun, S., Lawan, I., Wang, L., Lin, M., Yuan, Z. 2020. Preparation and evaluation of an effective activated carbon from white sugar for the adsorption of rhodamine B dye. J. Clean. Prod., 253, 119989.

Xiao, W., Jiang, X., Liu, X., Zhou, W., Garba, Z.N., Lawan, I., Wang, L., Yuan, Z. 2021. Adsorption of organic dyes from wastewater by metal-doped porous carbon materials. J. Clean. Prod., 284, 124773.